Does Reaction of Three-Coordinate Molybdenum(III) with N_2O Proceed via the Same Mechanism as with N_2? A Theoretical Study

Dmitry V. Khoroshun, Djamaladdin G. Musaev,* and Keiji Morokuma*

Cherry L. Emerson Center for Scientific Computation and Department of Chemistry, Emory University, Atlanta, Georgia 30322

Received May 24, 1999

Hybrid density functional (B3LYP) and integrated molecular orbital and molecular mechanics (IMOMM) calculations were performed to elucidate the mechanism of the reaction of nitrous oxide with the MoL_3 complex, where L = NH_2 and N[(^{t}Bu)(3,5-$C_6H_3Me_2$)], respectively. The first step of the reaction is coordination of N_2O to the Mo center of MoL_3, leading to the formation of $(N_2O)MoL_3$. From this complex, the reaction may proceeds via two distinct mechanisms, mononuclear and dinuclear. The mononuclear mechanism takes place via an N−N bond cleavage transition state and leads to formation of $NMo(NH_2)_3$ and free nitric oxide NO, which spontaneously reacts with another $Mo(NH_2)_3$ fragment, producing $(NO)Mo(NH_2)_3$. The dinuclear mechanism starts by coordination of another MoL_3 to (N_2O)-MoL_3, leading to formation of $L_3Mo(N_2O)MoL_3$, and splits further into two different paths, leading to N−O and N−N cleavage processes, among which the N−O activation is kinetically and thermodynamically more favorable. The experimental observation of the exclusive N−N cleavage is consistent only with the mononuclear mechanism. It was shown that inclusion of steric effects of the bulky amido ligands strongly favors the mononuclear mechanism by destabilizing the dinuclear reaction species much more than mononuclear species. The rate-determining step of the reaction of N_2O with bulky MoL_3 in the mononuclear mechanism is the N−N bond activation, which takes place with an 11 kcal/mol free energy of activation. Comparing these results with those for the reaction of N_2 with MoL_3 on one side and with available experiments on another side, we conclude that reactions of N_2O and N_2 with MoL_3 proceed via different mechanisms: nitrous oxide reacts with MoL_3 via a mononuclear mechanism, while dinitrogen reacts via a dinuclear mechanism.

I. Introduction

Understanding the mechanism of N≡N triple-bond activation and chemical transformations is of great fundamental and practical interest and has been the focus of extensive studies[1] during the last several decades. Despite all the efforts, many aspects of the nitrogen activation and transformation processes are not yet fully understood, and additional investigations are required. Recently, several important reactions that are believed to be relevant to various nitrogen fixation processes have been discovered. One of these extremely interesting reactions is cleavage of the N≡N triple bond of N_2[2] and N_2O[3] molecules by a three-coordinate complex of Mo, $Mo(NRAr)_3$ (R = $C(CH_3)_3$, Ar = 3,5-$C_6H_3Me_2$) reported by Cummins and co-workers.

It has been shown[2a] that purification of red-orange $Mo(NRAr)_3$ (ethyl ether, 0.1 M) under N_2 atmosphere at −35 °C leads to an intensively purple colored solution, which gradually became golden on warming to 30 °C and finally lost its paramagnetism. The ^{1}H NMR spectroscopy study confirmed that the final product is a terminal nitrido Mo(VI) complex, $NMo(NRAr)_3$. Formation of a dinuclear intermediate, $(NRAr)_3Mo(N_2)Mo(NRAr)_3$, at the early stages of the process has later been rigorously[2b] confirmed. In our previous quantum chemical studies[4] of the mechanism of N_2 cleavage by three-coordinate group 6 complexes ML_3 (where M = Cr, Mo, and W; L = H, Cl, NH_2, and OCH_3),[4] it has been confirmed that this reaction is a multistep process involving (i) coordination of the dinitrogen molecule to the transition metal center of the quartet ground state of the ML_3 complex to form a doublet $(N_2)ML_3$ inter-

(1) As leading references, see: (a) Ertl, G. In *Catalytic Ammonia Synthesis*; Jennings, J. R., Ed.; Plenum: New York, 1991. (b) Ludden, P. W. In *Encyclopedia of Inorganic Chemistry*; Wiley: New York, 1994; p 2566. (c) Coucouvanis, D. In *Encyclopedia of Inorganic Chemistry*; Wiley: New York, 1994; p 2557. (d) Howard, J. B.; Rees, D. C. *Chem. Rev.* **1996**, *96*, 2965. (e) Burgess, B. K.; Lowe, D. J. *Chem. Rev.* **1996**, *96*, 2983. (f) Eady, R. R. *Chem. Rev.* **1996**, *96*, 3013. (g) Leigh, G. J. *Science* **1998**, *279*, 506, and references therein. (h) Leigh, G. J. Acc. *Chem. Res.* **1992**, *25*, 177, and references therein. (i) Nishibayashi, Y.; Iwai, S.; Hidai, M. *Science* **1998**, *279*, 540, and references therein. (j) Fryzuk, M. D.; Love, J. B.; Rettig, S. J.; Young, V. G. *Science* **1997**, *275*, 1445.

(2) (a) Laplaza, C. E.; Cummins, C. C. *Science* **1995**, *268*, 861. (b) Laplaza, C. E.; Johnson, M. J. A.; Peters, J. C.; Odom, A. L.; Kim, E.; Cummins, C. C.; George, G. N.; Pickering, I. J. *J. Am. Chem. Soc.* **1996**, *118*, 8623.

(3) Laplaza, C. E.; Odom, A. L.; Davis, W. M.; Cummins, C. C. *J. Am. Chem. Soc.* **1995**, *117*, 4999−5000.

(4) (a) Cui, Q.; Musaev, D. G.; Svensson, M.; Sieber, S.; Morokuma, K. *J. Am. Chem. Soc.* **1995**, *117*, 12366. (b) Musaev, D. G.; Cui, Q.; Svensson, M.; Morokuma, K. Theoretical Studies of the N_2 Cleavage by Three-Coordinate Group 6 Complexes ML_3. In *Transition State Modeling for Catalysis*; Thruhlar, D. G., Morokuma, K., Eds.; ACS Symposium Series 721; American Chemical Society: Washington, DC, 1999.

10.1021/om990396r CCC: $18.00
Publication on Web 11/25/1999

Table 1. Calculated Bonding Energies (in kcal/mol) for L = NH_2 and N[(^{t}Bu)(3,5-$C_6H_3Me_2$)] at Various Levels[a]

	L = NH_2 pure MO (B3LYP)		L = N[(^{t}Bu)(3,5-$C_6H_3Me_2$)] IMOMM(B3LYP:MM3)		
structures	BSI	BSII	BSI	BSII	experiment
$N + N \rightarrow N_2$	−181.3/−189.6	−221.6/−229.6[b]			−217.7[c]
$N + O \rightarrow NO$	−116.1/−126.1	−150.7/−161.0[b]			−143.3[c]
$N_2 + O \rightarrow N_2O$	−31.6/−30.5	−45.6/−43.9[b]			−30.6[c]
$N + NO \rightarrow N_2O$	−96.7/−94.0	−116.5/−113.2[b]			−105.0[c]
$N + MoL_3 \rightarrow NMoL_3$	−127.9/−122.3	−142.1/−136.5	−120.6/−115.0	−135.5/−129.9	
$O + MoL_3 \rightarrow OMoL_3$	−130.8/−128.2	−145.9/−143.3	−123.0/−120.4	−138.3/−135.7	−155.6 ± 1.6[d]
$N_2 + MoL_3 \rightarrow (N_2)MoL_3$	−17.7 /−1.4	−4.0/+12.3	−9.0/+7.3	+0.2/+16.5	
$NO + MoL_3 \rightarrow (NO)MoL_3$	−75.9/−60.2	−71.0/−55.3	−70.4/−54.7	−66.3/−50.6	
$N_2O + MoL_3 \rightarrow (N_2O)MoL_3$	−28.5/−16.3	−14.4/−2.2	−21.3/−9.1	−7.2/+5.0	

[a] Numbers before and after "/" are the relative energies (without ZPC) and relative Gibbs free energies (298.15 K, 1 atm), where ZPC and entropy for the model system calculated at the B3LYP/BSI level were used for the other level and for the real system. [b] For these particular calculations, B3LYP/BS II entropy and ZP corrections were used. [c] Standard Gibbs energies of the reactions, calculated from data in ref 8. [d] Bond dissociation enthalpy from ref 9.

mediate, (ii) coordination of the second ML_3 fragment to the terminal nitrogen of $(N_2)ML_3$ to form a stable dinuclear complex, $L_3M(N_2)ML_3$, with a triplet ground state, (iii) crossover (spin flip) from the triplet to the singlet state of $L_3M(N_2)ML_3$, and (iv) N−N cleavage over a significant barrier to form product NML_3. We will below call this a *dinuclear* mechanism because of two transition metal atoms M involved in the reaction. We explored the dependence of the barrier to N−N bond cleavage on the nature of auxiliary ligands L and transition metal M, concluding that increase of π-donating capability of the ligand L decreases the energy gap between the triplet ground and singlet excited states of the dinuclear intermediate complex $L_3M(N_2)ML_3$, and, consequently, decreases the rate-determining barrier. These effects are even more pronounced for analogous W(III) complexes: a smaller energy gap between the ground s^1d^5 and excited s^2d^4 states for atomic W, 3.4 kcal/mol,[5] compared to that for atomic Mo, 34.0 kcal/mol,[5] puts the singlet state of $L_3M(N_2)ML_3$ only slightly (about 1 kcal/mol) above the triplet ground state. Consequently, the crossover from the triplet to singlet in the complex $L_3M(N_2)ML_3$ is more feasible. Additionally, the calculated rate-determining barrier is smaller and the exothermicity of the entire reaction is larger when M = W. We concluded[4] that WL_3 complexes with a strong π-donor ligand L would be more efficient in N_2 activation than the corresponding Mo(III) complex. This prediction is consistent with the fact that the C≡C bond in alkynes is cleaved easier by W complexes than by complexes of Mo.[6]

The present paper is a continuation of our previous studies and presents the results of our theoretical studies on the mechanism of reactions of the same $Mo(NRAr)_3$ complexes with N_2O. The experimental studies reported that exposure of degassed solutions of $Mo(NRAr)_3$ (0.157 mmol, 20 mL of ethyl ether, and 25 °C) to an excess (3−4 equiv) of N_2O resulted in production of the terminal nitrido complex $NMo(NRAr)_3$ and nitrosyl complex $(ON)Mo(NRAr)_3$ in a 1:1 ratio in over 10−15 min. No intermediate complexes were detected, and the diamagnetic $NMo(NRAr)_3$ and $(ON)Mo(NRAr)_3$ were the only significant products of the reaction. The latter finding is quite surprising, since one would expect (on the basis of the experience accumulated in inorganic chemistry[7]) the N_2O molecule to act as a source of oxygen atom. Indeed, in N_2O the N−O bond (bond energy = 30.6 kcal/mol, see Table 1)[8] is much weaker than the N≡N triple bond (105.0 kcal/mol).[8] At the same time, it is known that the Mo=O bond is comparable in strength to Mo≡N (both about 150 kcal/mol),[9] so that one would expect the N−O cleavage products to be at least equally, if not more, stable compared to products of N−N cleavage. Therefore, the exothermicity argument, used to explain the driving force of the analogous N_2 activation reaction,[4] cannot distinguish the two possible pathways for N_2O activation. The present paper is intended to (a) elucidate the possible mechanism of the reaction $N_2O + Mo(NRAr)_3$, (b) reveal the factors, both electronic and steric, determining the mechanism of this reaction, and (c) compare the results with those for the reaction with N_2. Namely, we studied the following reactions:

$$L_3Mo + N_2O + L_3Mo \rightarrow L_3Mo(N_2) + L_3Mo(O) \quad (I)$$

$$L_3Mo + N_2O + L_3Mo \rightarrow L_3Mo(N) + L_3Mo(NO) \quad (II)$$

for L = NH_2 and N[(^{t}Bu)(3,5-$C_6H_3Me_2$)], and we compared the results with those reported previously for the similar reaction with the N_2 molecule.

II. Computational Methods

First for the reactions of our model complex (all model species are denoted with **m**), MoL_3 with L = NH_2, we performed molecular orbital (MO) calculations. We used the B3LYP density functional method, with Becke's three-parameter hybrid exchange functional[10] in conjunction with Lee, Yang, and Parr's correlation functional.[11] Geometries of the stationary points on the potential energy surface of reactions

(5) Moore, C. E. *Atomic Energy Levels*; NSRD-NBS; U.S. Government Printing Office: Washington, DC, 1971; Vols. II and III.

(6) Murdzek, J. S.; Schrock, R. R. In *Carbyne Complexes*; Fischer, H., Hofmann, P., Keissl, F. R., Schrock, R. R., Schubert, U., Wiess, K., Eds.; VHS: New York, 1988; pp 147−203.

(7) (a) Vaughan, G. A.; Sofield, C. D.; Hillhouse, G. L.; Rheingold, A. L. *J. Am. Chem. Soc.* **1989**, *111*, 5491, and references therein. (b) Matsunaga, P. T.; Hillhouse, G. L.; Rheingold, A. L. *J. Am. Chem. Soc.* **1993**, *115*, 2075. (c) Arzoumanian, H.; Nuel, D.; Sanchez, J. *J. Mol. Catal.* **1991**, *65*, L9. (d) Bottomley, F. *Polyhedron* **1992**, *11*, 1707. (e) Smith, M. R.; Matsunaga, P. T.; Andersen, R. A. *J. Am. Chem. Soc.* **1993**, *115*, 7049. (f) Howard, W. A.; Parkin, G. *J. Am. Chem. Soc.* **1994**, *116*, 606.

(8) *CRC Handbook of Chemistry and Physics*; Lide, D. R., Frederikse, H. P. R., Eds.; CRC Press: Boca Raton, FL, New York, London, Tokyo, 1996.

(9) Johnson, A. R.; Davis, W. M.; Cummins, C. C.; Serron, S.; Nolan, S. P.; Musaev, D. G.; Morokuma, K. *J. Am. Chem. Soc.* **1998**, *120*, 2071.

I and II were optimized using a standard LANL2DZ basis set (denoted below as BSI), a double-ζ quality basis set[12] in conjunction with the Hay−Wadt relativistic effective core potential (ECP) for Mo atom.[13] Normal-mode analysis was carried out at the B3LYP/BSI level for all stationary points in order to verify their character by the number of imaginary frequencies (Nimag). Previously, we have demostrated[4] that the B3LYP/BSI approximation, used in this paper, gives reliable geometries for analogous systems. However, the calculated relative energies are usually more dependent on the basis sets and methods. Therefore, single-point energy calculations were performed for all of the B3LYP/BSI optimized structures at the B3LYP level with a larger basis set, BSII, including relativistic (28 electron) ECP of Dolg et al. associated with the (8s6p6d/6s4p3d) basis set for Mo[14] and the standard 6-31G*[15] basis for the other atoms. The zero-point vibrational energy correction (ZPC), thermal correction (at the 298.15 K), and entropy contribution (at 1 atm) to the energetics of the reactants, intermediates, transition states, and products of the reactions were calculated only at the B3LYP/BSI level and were used for all the energy calculations.

Second, for the reaction of the experimentally used system (species denoted with **r**) with bulky ligands, L = N[(ᵗBu)(3,5-$C_6H_3Me_2$)], we performed the integrated molecular orbital and molecular mechanics (IMOMM) calculations.[16] In the IMOMM method, a "model" system is cut from the "real" system, and this small model system is treated with an MO method, while the remainder of the real system is handled by an MM method. In the present calculation, the "model" system was chosen to be the electronically important parts, N_2O and $(NH_2)_3Mo$, which is the same as the system used in the pure MO calculations, and was treated with the B3LYP/BSI method. The actual ᵗBu and 3,5-$C_6H_3Me_2$ substituents were included into the "real system" (instead of hydrogen atoms of the model system) and treated with the MM3 force field[17] without the electrostatic contributions. The UFF van der Waals parameters by Rappé et al. were used for Mo atoms,[18] while all other MM contributions involving the metal atoms were set to zero. The IMOMM link bonds[16] were fixed at $R(N-H) = 1.0209$ Å, $R(N-C_{Ar}) = 1.4400$ Å, and $R(N-C_{sp^3}) = 1.4800$ Å. For the real system, we did not perform the normal coordinate analysis; we used the ZPC and the entropy correction of the "model" system at the B3LYP/BS I level as an estimate for the "real" system.

The MO calculations were carried out using the Gaussian94 package, supplemented with the analytical second derivative code.[19] IMOMM calculations were performed using the IMOMM[16a] code, which uses MM3(92)[17] and Gaussian92/DFT[10c] programs. All structures were optimized without symmetry constraints.

III. Results and Discussions

The sketches of structures and selected geometrical parameters of the calculated reactants, intermediates, transition states, and products of the reactions I and II are given in Figures 1 and 2. Cartesian coordinates of all optimized structures are given in the Supporting Information. Nimag values are shown only for transition states. Table 1 gives the bonding energies of some relevant species, and Table 2 the potential energies for the reactions I and II, calculated at all the levels of theory used, while below we will mainly discuss the energetics obtained at the B3LYP/BSII//B3LYP/BSI. The Gibbs free energies are calculated at the same, B3LYP/BSII//B3LYP/BSI, level of theory and at 298.15 K and 1 atm. In Scheme 1 we present the proposed "mononuclear" and "dinuclear" mechanisms of the reactions I and II. Discussion of the model system calculations is followed by the IMOMM results on the real system.

A. Reactant Complexes for the Model System. Let us start our discussions with the reactants of the reactions I and II. The reactant complex $Mo(NH_2)_3$, **1m,** has been discussed in our previous paper,[4] and the results will only be briefly summarized here. The ground state of this complex is the quartet $^4A_1'$, and the first excited doublet $^2A''$ state lies only 15.2 kcal/mol higher at the B3LYP/BSII level. Increase in π-donating capability of the auxiliary ligand decreases the doublet-quartet energy splitting of the ML_3 complex. In Figure 1, the optimized geometry of the ground quartet state of the $M(NH_2)_3$ complex is shown. The other reactant, N_2O, as seen in Figure 1, is linear in the singlet ground state.

The first step of reactions I and II is coordination of the N_2O molecule to the Mo center of L_3Mo, producing $L_3Mo(N_2O)$ four-coordinate complex. In general, the N_2O molecule can bind to Mo via either of its terminal atoms, N or O. Our calculation shows that O-approach is energetically unfavorable and results in no local minimum. Instead, the system without any barrier rearranges to the N-coordinated complex $(N_2O)Mo(NH_2)_3$, **2m** (Figure 1), whose ground state is doublet, with the quartet minimum lying about 15 kcal/mol higher. The calculated N_2O binding energy, i.e., that of the process $(N_2O)Mo(NH_2)_3$ (doublet) → $Mo(NH_2)_3$ (quartet) + N_2O (singlet), is 14.4 (2.2: Gibbs free energy, in parentheses hereafter) kcal/mol at the B3LYP/BII level, as shown in Table 1. In the doublet ground state of $(N_2O)Mo(NH_2)_3$, both N−N and N−O bonds of N_2O are elongated by 0.16 and 0.14 Å, respectively, from those in the free molecule. This can be compared with the N−N stretch of the N_2 molecule by only 0.04 Å upon coordination to $Mo(NH_2)_3$ (species **6m**, Figure 1). The 1.32 Å N−N bond length in **2m** has a character between a double and a single bond.

Such a significant weakening of the N−N bond in $(N_2O)Mo(NH_2)_3$ suggests that the N_2O activation reaction may easily take place via a mononuclear mechanism involving N−N cleavage immediately in **2m** (see Scheme 1). However, an analogy with the activation of the N_2 molecule suggests the dinuclear mechanism

(10) (a) Becke, A. D. *Phys. Rev. A* **1988**, *38*, 3098. (b) Becke, A. D. *J. Chem. Phys.* **1993**, *98*, 5648. (c) Frisch, M. J.; Trucks, G. W.; Schlegel, H. B.; Gill, P. M.; Johnson, B. G.; Wong, M. W.; Foresman, J. B.; Robb, M. A.; Head-Gordon, M.; Replogle, E. S.; Gomperts, R.; Andres, J. L.; Raghavachari, K.; Binkley, J. S.; Gonzalez, C.; Martin, R. L.; Fox, D. J.; Defrees, D. J.; Baker, J.; Stewart, J. J. P.; Pople, J. A. *Gaussian 92/DFT*; Gaussian Inc.: Pittsburgh, PA, 1993.
(11) Lee, C.; Yang, W.; Parr, R. G. *Phys. Rev. B* **1988**, *37*, 785.
(12) Dunning, T. H., Jr.; Hay, P. J. In *Modern Theoretical Chemistry*; Schaefer, H. F., III, Ed.; Plenum: New York, 1977; Vol. 3, pp 1−27.
(13) Hay, P. J.; Wadt, W. R. *J. Chem. Phys.* **1985**, *82*, 299.
(14) Andrae, D.; Haeussermann, U.; Dolg, M.; Stoll, H.; Preuss, H. *Theor. Chim. Acta* **1990**, *77*, 123.
(15) (a) Hehre, W. J.; Ditchfield, R.; Pople, J. A. *J. Chem. Phys.* **1972**, *56*, 2257. (b) Hariharan, P. C.; Pople, J. A. *Theor. Chim. Acta* **1973**, *28*, 213.
(16) (a) Maseras, F.; Morokuma, K. *J. Comput. Chem.* **1995**, *16*, 1170. (b) Matsubara, T.; Maseras, F.; Koga, N.; Morokuma, K. *J. Phys. Chem.* **1996**, *100*, 2573. (c) Matsubara, T.; Sieber, S.; Morokuma, K. *Int. J. Quantum Chem.* **1996**, *60*, 1101.
(17) (a) MM3(92): Quantum Chemistry Program Exchange, Indiana University, 1992. (b) Aped, A.; Allinger, N. L. *J. Am. Chem. Soc.* **1992**, *114*, 4, 1.
(18) Rappe, A. K.; Casewit, C. J.; Colwell, K. S.; Goddard, W. A., III; Skiff, W. M.; *J. Am. Chem. Soc.* **1992**, *114*, 10024.
(19) Cui, Q.; Musaev, D. G.; Svensson, M.; Morokuma, K. *J. Phys. Chem.* **1996**, *100*, 10936.

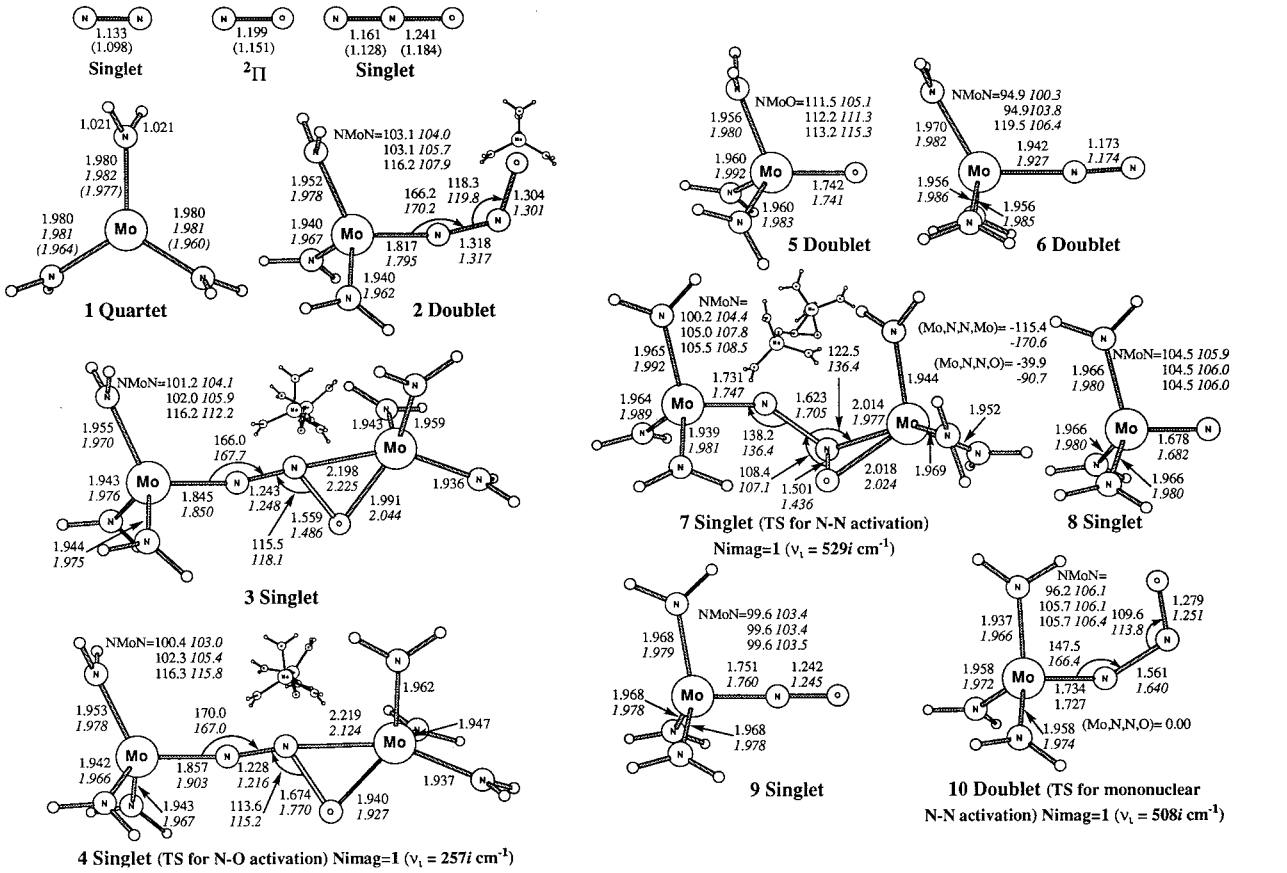

Figure 1. Geometries of the reactants, intermediates, transition states, and products of the reactions I and II for L = NH_2 (model, **m**) and N[(^{t}Bu)(3,5-$C_6H_3Me_2$)] (real, **r**, in italic) calculated at the B3LYP/BSI level. Distances are given in Å, and angles are given in deg. Experimental values, when available, are shown in parentheses. Nimag and the value of the imaginary frequency are calculated only for the model system. Only ground spin state minima parameters are given. Full Cartesian coordinates of all optimized structures are given in the Supporting Information.

(again see Scheme 1). We will examine the dinuclear mechanism first, followed by discussion of the mononuclear mechanism.

B. Dinuclear Mechanism. The dinuclear mechanism will be initiated by coordination of the second MoL_3 fragment to $(N_2O)Mo(NH_2)_3$, giving a dinuclear intermediate, $(NH_2)_3Mo(N_2O)Mo(NH_2)_3$, which is followed by either N−N or N−O bond activation, leading to the $NMo(NH_2)_3 + (NO)Mo(NH_2)_3$ or $OMo(NH_2)_3 + (N_2)Mo(NH_2)_3$ products, respectively.

The first step is coordination of $Mo(NH_2)_3$ to $(N_2O)Mo(NH_2)_3$ to form a dinuclear complex, $(NH_2)_3Mo(N_2O)Mo(NH_2)_3$, **3m** in Figure 1. Since the ground states of $(N_2O)Mo(NH_2)_3$ and $Mo(NH_2)_3$ are doublet and quartet, respectively, the produced dinuclear complex may be either quintet or triplet; conversion to the singlet state requires a spin flip. The ground state of $(NH_2)_3Mo(N_2O)Mo(NH_2)_3$ is singlet, and the triplet state is only 2.2 kcal/mol higher (at the B3LYP/BSI level). The quintet state is antibonding and was not studied. Below we will discuss in detail only the singlet state, the only state that connects to both doublet + doublet products after N−O cleavage and singlet + singlet products after N−N fission.

Coordination of the second $Mo(NH_2)_3$ to $(N_2O)Mo(NH_2)_3$ is calculated to be exothermic by 50.3 (33.0) kcal/mol. As seen in Figure 1, upon coordination of the second $Mo(NH_2)_3$, the N−N bond is shortened by 0.08 Å, while the N−O bond is elongated by 0.26 Å. The N−O bond (1.56 Å) in **3m** is already longer than an N−O single bond (e.g., 1.45 Å in NH_2−OH). At the same time,

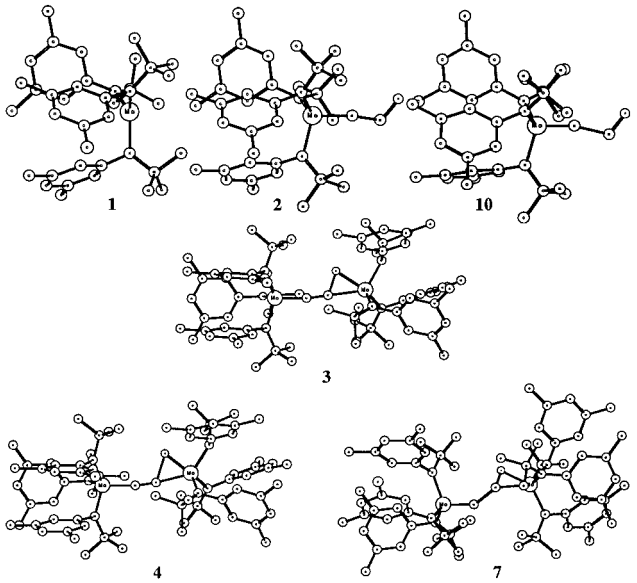

Figure 2. Optimized structures of the initial complex **1r** (quartet ground state), mononuclear complex **2r** (doublet), mononuclear N−N cleavage TS **10r** (doublet), dinuclear complex **3r**, and N−O and N−N cleavage TSs **4r** and **7r** (all singlets). Hydrogen atoms are omitted for clarity. Full Cartesian coordinates of all optimized structures are given in the Supporting Information.

Table 2. Relative Energies (relative to the ground quartet state of reactants: 1 + N_2O, in kcal/mol) of the Reactions I and II for L = NH_2 and N[(^{t}Bu)(3,5-$C_6H_3Me_2$)] Calculated at Different Levels[a]

		model, L = NH_2 pure MO (B3LYP)		**real**, L = N[(^{t}Bu)(3,5-$C_6H_3Me_2$)] IMOMM(B3LYP:MM3)	
structures	multiplicity	BSI	BSII	BSI	BSII
reactants, MoL_3 **1** + NO	Q	0.0	0.0	0.0	0.0
	D	14.4	15.2	15.5	
$(N_2O)MoL_3$, **2**	D	−28.5/−16.3	−14.4/−2.2	−21.3/−9.1	−7.2/+5.0
		Dinuclear Mechanism			
$L_3Mo(N_2O)MoL_3$, **3**	S	−76.7/−47.2	−64.7/−35.2	−50.0/−20.5	−36.5/−7.0
TS (N−O cleavage), **4**	S	−76.3/−47.0	−61.2/−31.9	−46.3/−17.0	−31.3/−2.0
barrier from ***3***		*0.4/0.2*	*3.5/3.3*	*3.7/3.5*	*5.2/5.0*
$OMoL_3 + (N_2)MoL_3$		−116.9/−99.1	−104.3/−86.5	−100.4/−82.6	−92.5/−74.7
TS (N−N cleavage), **7**	S	−55.5/−27.3	−39.6/−11.4	−23.4/+4.8	−11.2/+17.0
barrier from ***3***		*21.2/19.9*	*25.1/23.8*	*26.6/25.3*	*25.3/24.0*
$NMoL_3 + (NO)MoL_3$		−107.1/−88.5	−96.6/−78.0	−94.3/−75.7	−85.3/−66.7
		Mononuclear Mechanism			
TS (N−N cleavage), **10**		−19.4/−8.9	−3.7/+6.8	−14.8/−4.3	+0.2/+10.7
barrier from ***2***		*9.1/7.4*	*10.7/9.0*	*6.5/4.8*	*7.4/5.7*
$NMoL_3 + NO$		−31.0/−30.0	−25.6/−24.6	−23.8/−22.8	−19.1/−18.1

[a] Numbers before and after "/" are the relative energies (without ZPC) and relative Gibbs free energies (298.15 K, 1 atm), where the ZPC and entropy for the model system calculated at the B3LYP/BSI level were used for the other level and for the real system. In italic are barriers from the corresponding prereaction complexes. Multiplicities are singlet (S), doublet (D), and quartet (Q).

Scheme 1. Schematic Representation of the Proposed "Mononuclear" and "Dinuclear" Mechanisms of the Reaction of MoL_3 with Nitrous Oxide, N_2O

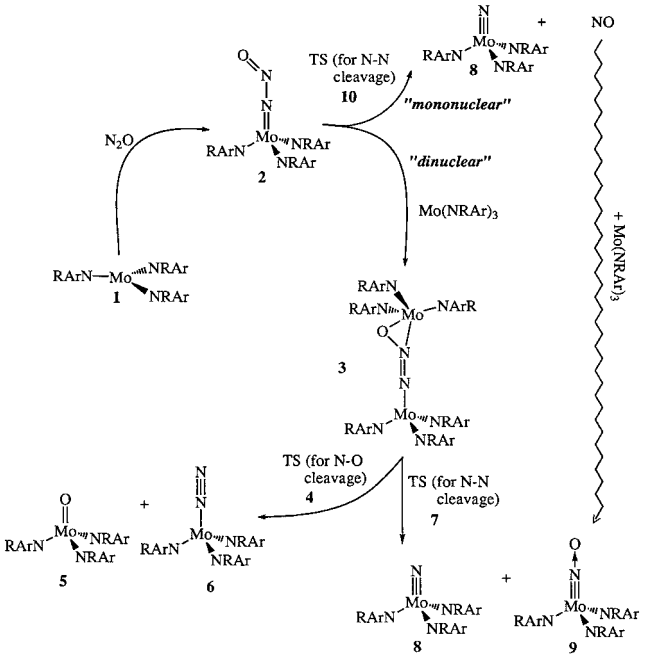

(a) the N−N bond becomes stronger (formally a double bond, 1.243 Å); (b) a strong Mo−O bond (1.991 Å) is formed, and (c) the N_2 fragment is bound mainly to one of two Mo atoms (Mo−N bond distances 1.845 and 2.198 Å). All these geometry changes clearly indicate that complex **3m** may be regarded in part as a complex between $OMo(NH_2)_3$ and $(N_2)Mo(NH_2)_3$.

From **3m**, the reaction splits into two paths, as seen in Scheme 1. The first of them is activation of the N−O bond. According to the results presented in Table 2, N−O bond activation in **3m** takes place quite easily via a transition state **4m**, with the barrier being only 3.5 (3.3) kcal/mol. Structure **4m** is a real transition state with one imaginary frequency of 257i cm^{-1} corresponding to the N−O stretch. Going form **3m** to **4m**, the N−O bond is elongated from 1.559 Å to 1.674 Å, while the Mo−O, Mo−N, and N−N bonds do not change significantly. Obviously, from both structural and energetical points of view the transition state **4m** is quite an early one. Overcoming this small barrier leads to formation of the products, $OMo(NH_2)_3$, **5m**, and $(N_2)Mo(NH_2)_3$, **6m**. This process is calculated to be exothermic by 104.3 (86.5) and 39.6 (51.1) kcal/mol relative to the reactants, $2Mo(NH_2)_3$(quartet) + N_2O, and the immediate precursor, **3m**, respectively.

The second pathway originating at complex **3m** is the N−N activation through the transition state **7m**, leading to the experimentally observed products, $NMo(NH_2)_3$, **8m**, and $(NO)Mo(NH_2)_3$, **9m**. The transition state **7m** has one imaginary frequency of 529i cm^{-1} corresponding to the N−N stretching. As seen from Figure 1, the N−N bond is stretched from 1.243 Å in **3m** to 1.623 Å in TS **7m**. At the same time, two different Mo−N bonds shorten from 1.845 and 2.196 Å in **3m** to 1.731 and 2.014 Å in TS **7m**, respectively. The Mo−O and N−O bond distances change only slightly. All these geometry changes once again confirm the nature of the TS **7m**. The calculated barrier height is 25.1 (23.8) kcal/mol relative to structure **3m**. Past the transition state **7m** lie the experimentally observed products, $NMo(NH_2)_3$, **8m**, and $(NO)Mo(NH_2)_3$, **9m**, 96.6 (78.0) and 31.9 (42.8) kcal/mol lower in energy than the reactants $2Mo(NH_2)_3$(quartet) + N_2O, and complex **3m**, respectively.

Comparing the two different pathways starting from the complex **3m**, namely, N−O and N−N bond activation of the N_2O moiety, we conclude that (1) kinetically the N−O activation process, occurring with a 3.5 (3.3) kcal/mol barrier, is much easier than N−N activation, which requires passing over a 25.1 (23.8) kcal/mol barrier, and (2) the products $OMo(NH_2)_3$ + $(N_2)Mo(NH_2)_3$ of the N−O bond activation process are thermodynamically more stable than the products $NMo(NH_2)_3$ + $(NO)Mo(NH_2)_3$ of N−N bond activation. In other words, the dinuclear mechanism discussed above kinetically and thermodynamically favors N−O over N−N bond activation. This conclusion contradicts the experi-

mentally observed *exclusive* N−N bond cleavage in the reaction of MoL_3 with N_2O. The only products characterized experimentally are $NMoL_3$, **8**, and $(NO)MoL_3$, **9**, corresponding to the N−N bond cleavage in the N_2O molecule.

Thus, the dinuclear mechanism for the reaction of MoL_3 with N_2O is not acceptable, and we should look for another, more appropriate pathway. One of such possibilities is the above-mentioned mononuclear mechanism.

C. Mononuclear Mechanism. As has been described above (Scheme 1), mononuclear and dinuclear mechanisms have a common intermediate, doublet $(N_2O)MoL_3$ complex, **2**. The mononuclear mechanism proceeds further by a unimolecular N−N bond activation via a transition state, **10**, producing one of the experimentally observed products, $NMoL_3$, **8**, and a molecule of nitric oxide NO. Immediately, free NO and another MoL_3 radical will form without barrier the second experimentally observed product, $(NO)MoL_3$, **9**.

As seen in Figure 1, the N−N cleavage transition state, **10m**, has only one imaginary frequency (508i cm^{-1}) corresponding to the N−N stretching reaction coordinate. In **10m**, the N−N bond distance is elongated significantly from 1.318 Å in **2m** to 1.561 Å. Meanwhile, the Mo−N bond shortens from 1.817 Å in **2m** to 1.734 Å. The N−O bond distance does not change significantly. All these geometrical differences between TS **10m** and reactant **2m** clearly indicate that this transition state indeed corresponds to formation of $NMo(NH_2)_3$, **8m**, and free NO molecule. The calculated barrier height of this process is only 10.7 (9.0) kcal/mol relative to **2m**. Products of this reaction, **8m** and free NO molecule, lie 25.6 (24.6) and 11.2 (22.4) kcal/mol lower than reactants $Mo(NH_2)_3 + N_2O$ and the immediate precursor, **2m**, respectively.

Let us now compare the results between mononuclear and dinuclear mechanisms. The common intermediate for both mechanisms is the complex $(N_2O)MoL_3$, **2m**. In the mononuclear mechanism, **2m** will react unimolecularly over the TS **10m** at the rate of k_m[**2**], which has an activation free energy of 9.0 kcal/mol. On the other hand, in the binuclear mechanism, **2m** will react with the second MoL_3 to form a binuclear intermediate **3m** at the rate of k_b[**2**][MoL_3] depending on the concentration of MoL_3, which in turn is dependent on the diffusion of the complex. The bimolecular rate constant k_b is expected to have very little, if any, activation free energy. The mononuclear mechanism, after going over the TS **10m**, exclusively gives the N−N cleavage products, $NMoL_3$, **8m**, and $(NO)MoL_3$, **9m**, observed by experimentalists.[3] The dinuclear mechanism, from intermediate **3m**, prefers the cleavage of the N−O bond with a small activation free energy of 3.3 kcal/mol to give the products $OMoL_3$, **5m**, and $(N_2)MoL_3$, **6m**. The N−N cleavage in the dinuclear mechanism is very unfavorable.

D. Influence of Bulky Ligands. The bulky ligands L = N[(^{t}Bu)(3,5-$C_6H_3Me_2$)] present in the actual system certainly introduce some so-called "steric effects", which may favor one over the other mechanism described above. In particular, one may expect the steric effects to favor the mononuclear mechanism, because of the potentially strong ligand−ligand repulsion which may destabilize the dinuclear complex **3**. All the previous discussions were based on the results obtained for the reaction of a *model* complex $Mo(NH_2)_3$ with N_2O. In other words, the steric effects from the bulky substituents of the ligand were absent in these results. To take into account the steric effects, we performed more realistic calculations, which explicitly incorporated the experimentally used bulky ligand N[(^{t}Bu)(3,5-$C_6H_3Me_2$)]. In this section, we will discuss results of these integrated molecular orbital + molecular mechanics (IMOMM) studies of the reactions I and II for the complex $Mo\{N[(^t Bu)(3,5\text{-}C_6H_3Me_2)]\}_3$. Sketches of some important optimized structures of the reactants, intermediates, and products of the reactions I and II are shown in Figure 2. Some of the important geometrical parameters are shown in Figure 1, and the energies in Tables 1 and 2, along with those for the corresponding model systems.

First, we would like to very briefly point out the changes in the geometries due to the steric effects. In general, as seen in Figure 1, by replacing the NH_2 ligands on the model system $Mo(NH_2)_3$ by the bulky N[(^{t}Bu)(3,5-$C_6H_3Me_2$)] ligands, geometries of the complexes MoL_3 **1**, $NMoL_3$ **8**, $OMoL_3$ **5**, $(N_2)MoL_3$ **6**, $(NO)MoL_3$ **9,** and $(N_2O)MoL_3$ **2** change only slightly, and we will not discuss these in detail. However, changes in important geometric parameters of the dinuclear complex **3**, as well as of the transition states **4**, **7**, and **10**, are significant and worth discussing. As seen from Figure 1 for the complex **3**, upon going from the model to the real system, the Mo−O and the Mo−N bond for the second Mo (right in Figure 1) are elongated from 1.991 Å to 2.044 Å and from 2.198 Å to 2.225 Å, while the N−O bond is shortened from 1.559 Å to 1.486 Å. One can conclude that the interaction between the $L_3Mo(NNO)$ complex and the second MoL_3complex is weakened substantially. For transition states **4** and **7** these changes are even larger. For TS **4**, TS for N−O bond activation process (from **3** to **5**+**6**), introduction of the bulky N[(^{t}Bu)(3,5-$C_6H_3Me_2$)] ligands shortens the forming Mo−O bond from 1.940 Å to 1.927 Å and elongates the breaking N−O bond from 1.674 Å to 1.770 Å, respectively, while the N−N bond is shortened slightly by 0.012 Å. These changes suggest that the bulky N[(^{t}Bu)(3,5-$C_6H_3Me_2$)] ligands make the TS **4** later or more product-like. Similarly the N−N cleavage TS **7** (from **3** to **8**+**9**) also became relatively late with the bulky N[(^{t}Bu)(3,5-$C_6H_3Me_2$)] ligands. The breaking N−N bond is elongated from 1.623 Å to 1.705 Å, while the forming Mo−N bond and the N−O bond are shortened from 2.014 Å to 1.977 Å and from 1.501 Å to 1.436 Å, respectively, all more like the products. On the other hand, the geometry changes in the monomeric N−N cleavage TS **10** are relatively small. A substantial change occurred only in the length of the breaking N−N bond, which increased from 1.561 Å in the model system to 1.640 Å in the real system, again suggesting a later transition state. Geometrical parameters of a less sterically crowded mononuclear TS **10r** are less dependent on bulkiness of the ligands compared to more crowed dinuclear TSs **4r** and **7r**.

As seen from Table 2, which compares the energetics between the model (**m**) and the real (**r**) system, the bulky ligands in general destabilize intermediates,

transition states, and products relative to the reactants ($2MoL_3$ **1** + NO_2). In particular, the energies of all dinuclear species (**3**, TS **4**, and TS **7**) are shifted up by 25−30 kcal/mol, apparently due to both *interfragment* steric repulsion between the ^{t}Bu groups and *intrafragment* repulsion between Ar groups. On the other hand, each four-coordinate mononuclear species (**(**N_2O)MoL_3, $OMoL_3$, (N_2)MoL_3, $NMoL_3$, (NO)MoL_3, and TS **10**) is destabilized by 5−7 kcal/mol, because of the *intrafragment* steric interaction among the Ar and ^{t}Bu groups, which is more pronounced than in the three-coordinate reactant MoL_3, where the MoNNN moiety is nearly coplanar.

Moreover, the presence of the bulky ligands on the MoL_3 fragments results in several important mechanistic implications that we would like to point out explicitly. First, the bulky ligands destabilize (N_2O)-MoL_3 **2** by about 7 kcal/mol, and consequently, the calculated complexation energy for N_2O + MoL_3 → (N_2O)MoL_3 (**2r**) (see Table 1) becomes −7.2 (+5.0) kcal/mol, where "+" in the Gibbs free energy means that the complex is unstable relative to the dissociation limit. This is consistent with the experimental fact that no intermediate is observed for the actual system. Second, introduction of the bulky ligands reduces the energy difference between species (N_2O)MoL_3 (**2r**) and transition state **10r** by 3−4 kcal/mol, from 10.7 (9.0) to 7.4 (5.7) kcal/mol. Analysis of the components of combined IMOMM energies reveals that deformation of the model system ($Mo(NH_2)_3$) in the produced IMOMM minimum **2r** is responsible for both changes. Namely, our model system structure **2m** contains an NH_2 group perpendicular to the MoN_2O plane (see Figure 1), which allows for "push−pull" donation of electron density from the nitrogen's lone pair through the occupied d_{xz} orbital of Mo further to the π^* orbitals of N_2O, enhancing back-donation and increasing the N_2O binding energy. Such a back-donation is much less important for the transition state **10**, which lacks the π^* system; therefore, the effect of bulky substituents, which make the electronically favorable "perpendicular" orientation of NRAr groups prohibitively sterically unfavorable (see Figure 2), is much more pronounced for **2** compared with **10**. Due to steric effects, the former (L_3MoN_2O complex **2**) is destabilized more strongly than the latter (N−N cleavage TS **10**).

Summarizing the effects of the bulky substituents on the reaction energetics, the initial N_2O coordination, N_2O + MoL_3 → (N_2O)MoL_3 (**2**), while exothermic (free energy change of −2.2 kcal/mol) for model (**m**), becomes endothermic (+5.0 kcal/mol) for real (**r**). The free energy of the mononuclear N−N cleavage TS (**10**) relative to the immediate precursor, complex (N_2O)MoL_3 (**2**), is reduced from 9.0 kcal/mol for model (**m**) to 5.7 kcal/mol for real (**r**). Since the formation of the transient (N_2O)-MoL_3 and the N−N cleavage are expected to take place in one activation step, we argue that the overall activation free energy is 5.0 + 5.7 = 10.7 kcal/mol. On the other hand, the bimolecular process, MoL_3 + (N_2O)MoL_3 (**2**) → $L_3Mo(N_2O)MoL_3$ (**3**), highly (−33.0 kcal/mol) exothermic for model (**m**), is only modestly (−12.0 kcal/mol) exothermic for real (**r**). The N−N activation from the dinuclear complex, $L_3Mo(N_2O)MoL_3$ (**3**), remains unfavorable (24.0 kcal/mol activation free energy). The activation free energy for the N−O cleavage of the dinuclear complex, $L_3Mo(N_2O)MoL_3$ (**3**) → TS **4**, is increased from 3.3 kcal/mol for model (**m**) to 5.0 kcal/mol for real (**r**).

The overall rate of the dinuclear mechanism is expected to be determined by the rate of the bimolecular process, MoL_3 + (N_2O)MoL_3 (**2**) → $L_3Mo(N_2O)MoL_3$ (**3**), which will depend on the diffusion rate of the two complexes. The diffusion is expected to be very slow for complexes with bulky ligands in the real (**r**) system. However, it is very clear from the present calculations that introduction of the bulky ligands favors the mononuclear mechanism energetically and diffusionally over the dinuclear mechanism. The experimental observation of the exclusive N−N cleavage, which is attributed based on the present calculations to the mononuclear mechanism, may in fact be due to the existence of bulky ligands. Less bulky ligands may give N−O cleavage via the dinuclear mechanism.

IV. Conclusions

We may draw the following conclusions from the above results and discussions.

1. The reaction of the model complex $Mo(NH_2)_3$ with nitrous oxide starts with coordination of the N_2O molecule to the Mo center, leading to the formation of the (N_2O)$Mo(NH_2)_3$ complex. This complex is a branching point for two pathways, mononuclear and dinuclear. The mononuclear mechanism is a unimolecular process independent of diffusion, takes place with a small (9 kcal/mol) N−N bond cleavage barrier at the transition state **10**, and leads to formation of complex $NMo(NH_2)_3$ and free nitric oxide NO, which reacts barrierlessly with another $Mo(NH_2)_3$ fragment to give the nitrosyl complex (NO)$Mo(NH_2)_3$. In contrast, the dinuclear mechanism, which starts by coordination of another $Mo(NH_2)_3$ fragment to the (N_2O)$Mo(NH_2)_3$ to form dinuclear intermediate **3**, results in N−O cleavage (with smaller than 5 kcal/mol barrier) rather than N−N cleavage (with larger than 20 kcal/mol barrier). Formation of the dinuclear intermediate **3** is highly exothermic (by about 30 kcal/mol), but at the same time is a bimolecular process and is associated with the diffusion of complexes. Although it is not straightforward to compare the rates of the two mechanisms, the experimental observation of the exclusive N−N cleavage is consistent only with the mononuclear mechanism.

2. Introduction of bulky substituents on the imido ligand L on the MoL_3 fragment destabilizes (N_2O)MoL_3 and makes it thermodynamically unstable to the dissociation limit: N_2O + MoL_3. This is consistent with no experimental observation of such intermediate. Bulky ligands increase the probability of the mononuclear mechanism over the dinuclear mechanism. The bulky ligands lower the rate-determining N−N cleavage barrier in the mononuclear mechanism. On the other hand, the bulky ligands make the MoL_3 + (N_2O)MoL_3 coordination process in the dinuclear mechanism much less exothermic and are expected to reduce the diffusion of the complexes, which determines the rate of this bimolecular process. Decreasing the steric bulk on the amido ligands may allow for realization of the dinuclear mechanism, resulting in N−O rather than N−N cleavage. A straightforward comparison of the calculated

rates between the mononuclear mechanism and the dinuclear mechanism for the bulky system seems to suggest that the dinuclear mechanism is energetically more favorable, which is inconsistent with the experimental observation of N−N cleavage product. The inconsistency may result from the missing transition state between $MoL_3 + (N_2O)MoL_3$ (**1r + 2r)** and MoL_3-$(N_2O)MoL_3$ (**3r**) for the dinuclear mechanism, which will be a focus of our future study.

3. Comparison of these conclusions with those obtained for the reaction of N_2 with MoL_3 in our previous theoretical studies[4] indicates that reactions of N_2O and N_2 with bulky MoL_3 proceed via different mechanisms; nitrous oxide reacts with MoL_3 via a mononuclear mechanism, while dinitrogen reacts via the dinuclear mechanism.

Acknowledgment. The authors express their gratitude to Prof. C. C. Cummins for bringing this problem to their attention and for very useful and intensive discussions. Discussions with Dr. Feliu Maseras on the details of IMOMM methodology are also highly appreciated. The use of computational facilities at the Emerson Center at Emory University, Maui High Performance Computer Center (MHPCC), and National Center for Supercomputing Applications (NCSA) is acknowledged. The present research is in part supported by a grant (CHE-9627775) from the National Science Foundation.

Supporting Information Available: Tables of Cartesian coordinates of all the optimized structures. This material is available free of charge via the Internet at http://pubs.acs.org.

OM990396R